ELSEVIER

Catalysis Today 65 (2001) 157–162

CATALYSIS TODAY

www.elsevier.com/locate/cattod

Synthesis of platinum–tin/alumina reforming catalysts from a well-defined platinum–tin precursor complex

C. Audo [a,*], J.F. Lambert [a], M. Che [a,b], B. Didillon [c]

[a] *Laboratoire de Réactivité de Surface, UMR 7609-CNRS, Université Pierre et Marie Curie, 4, Place Jussieu, Casier 178, 75 252 Paris Cedex 05, France*

[b] *Member of the Institut Universitaire de France, France*

[c] *Institut Français du Pétrole, 1-4 Av. du Bois Préau, 92 852 Rueil-Malmaison, France*

Abstract

The complex $[(CH_3)_4N]_3[Pt(SnCl_3)_5]$ was selected as a molecular precursor to prepare $PtSn/\gamma_c$-Al_2O_3 reforming catalysts. The spectroscopic fingerprints of the starting complex were obtained by ^{195}Pt and ^{119}Sn NMR and diffuse reflectance UV–visible spectroscopy. A series of supported catalysts were synthesized by wet impregnation of alumina with a solution of the precursor in acetone.

Well-dispersed species are obtained for Pt loadings below 1 wt.%; at higher loadings, a second species is formed that has spectroscopic features reminiscent of the initial complex and precipitates as a separate phase. Apparently, the Pt–Sn bonds are hydrolyzed in the low-loading species and preserved in the high-loading species.

The thermal transformations of $PtSn/\gamma_c$-Al_2O_3 catalysts are also studied and compared with those of the bulk precursor. In particular, it is shown that the nature of the atmosphere of thermal treatment (neutral or oxidizing) can orient the final catalyst towards preservation of an intimate Pt–Sn interaction, or towards demixtion.

Keywords: Reforming; Preparation; $[(CH_3)_4N]_3[Pt(SnCl_3)_5]$; Catalysts; $Pt–Sn/Al_2O_3$; NMR of ^{119}Sn; NMR of ^{195}Pt

1. Introduction

Pt-based reforming catalysts have evolved considerably since their first use in the late 1940s. In the late 1960s, the monometallic Pt/γ_c-Al_2O_3 catalyst was replaced by bimetallic $Pt–M/\gamma_c$-Al_2O_3 systems with M = Ge, Re, Ir or Sn [1]. The introduction of a second metal confers better stability and selectivity to the working catalyst [2] and allows to carry out reforming at lower pressures. The three major bimetallic catalysts used today are Pt–Re [3], Pt–Ir [4] and Pt–Sn [5–7].

The addition of Sn changes the catalytic selectivity by decreasing the hydrogenolysis reactions and the rate of carbon deposition and by boosting the selectivity towards aromatics during paraffin dehydrocyclization [8]. This effect has been explained in different ways. Dautzenberg et al. [9] and Biloen et al. [10] have suggested that Sn plays the role of an active phase "thinner" leading to smaller Pt metallic particles (geometric, ensemble effect). Burch [11], instead, has proposed that Sn modifies the electronic properties of the small Pt particles.

$Pt–Sn/Al_2O_3$ can be prepared by different methods: successive impregnations, co-impregnation, "wet" or incipient wetness impregnation. The choice of metal precursors is limited; most often, H_2PtCl_6 is used as

* Corresponding author. Tel.: +33-144-2755-59; fax: +33-144-2760-33.
E-mail address: audo@ccr.jussieu.fr (C. Audo).

0920-5861/01/$ – see front matter
PII: S0920-5861(00)00589-7

the Pt precursor and $SnCl_2$ or $SnCl_4$ as the Sn precursor. However, the interest for bimetallic catalysts has led to search for new preparation procedures and new catalyst designs. For example, sol–gel methods have been applied by Gomez et al. [12] and Bettcher et al. [13]. More relevant to the present work are studies using well-defined coordination compounds as Pt and Sn precursors, and a preformed alumina support. One can distinguish compounds with no direct Pt–Sn bond such as $[Pt(NH_3)_4][SnCl_6]$ [14] or $[Pt(NH_3)_4][SnCl_4]$ [15] from those that contain at least one such bond, for instance $[PtCl_2(SnCl_3)_2]^{2-}$ [16–18], $[PtCl(SnCl_3)(PPh_3)_2]$ [19], $[Pt_3Sn_8Cl_{20}]^{4-}$ [20], or $[Pt_3Sn_2Cl_6(NBD)_3]$ [21].

Using the latter approach, we have selected the coordination complex $[Pt(SnCl_3)_5]^{3-}$ as precursor containing the three elements (Pt, Sn and Cl) found in reforming catalysts and five direct Pt–Sn bonds. This complex has been used previously in the study of reforming catalysts by Yermakov et al. [22] and Li et al. [23]. These authors investigated the catalyst activity and selectivity in dehydrocyclization reactions but did not characterize the supported species along the successive preparation steps. On the other hand, we wanted to follow the evolution of the Pt–Sn complexes starting from the impregnation solution up to the active reforming catalysts, by a molecular-level characterization of the system after each preparation step. In particular, we tried to determine if the existence of a Pt–Sn bond in the initial precursor complex has an influence on the intimacy of the Pt–Sn interaction throughout the successive steps of catalyst preparation.

2. Experimental

2.1. Preparation of catalysts

The $[(CH_3)_4N]_3[Pt(SnCl_3)_5]$ precursor complex was synthesized and recrystallized along the method of Antonov et al. [24]. The support used was a γ_c-alumina provided by IFP with a BET surface area of $200\,m^2\,g^{-1}$ and a pore volume of $0.7\,ml\,g^{-1}$.

The catalysts were prepared by wet impregnation of the support with an acetone solution of the precursor salt (the metal complex is only stable in aqueous solutions at very low pHs). The solvent was removed under vacuum. Five samples were investigated with different Pt loadings of 0.5, 1, 1.5, 2 and 3 wt.%.

Two types of thermal treatment were carried out after drying: calcination under dry air flow or treatment under Ar flow (both $20\,ml\,min^{-1}$, 2 h at 773 K).

2.2. Characterization of catalysts

Powder X-ray diffraction patterns of powders were collected using a Siemens D-500 X-ray diffractometer equipped with a graphite monochromator and a Cu target, with a step width of 0.02° 2θ and a counting time of 2 s. The apparatus was connected to a DACO-MP microprocessor and the Diffract-AT software was used to analyze the data.

UV–visible spectra were collected in the 190–900 nm range, using a Cary 5 spectrometer working in the reflectance mode.

^{119}Sn and ^{195}Pt NMR spectra were obtained on an MSL-400 spectrometer from Brüker, operating at Larmor frequencies of 85.996 MHz for ^{195}Pt and 149.089 MHz for ^{119}Sn. Simple 1-pulse excitations were used, with pulse lengths of 4 μs and recycle delays of 10 s. Liquid-state and MAS NMR spectra were recorded using standard Brüker probes, with zirconia rotors spinning at 10 kHz for MAS spectra. Sn and Pt chemical shifts are expressed relative to external $SnMe_3$ and 0.2 M aqueous H_2PtCl_6, respectively.

Thermogravimetric and differential thermal analyses (TGA, DTA) were performed on a Seiko SSC 5200H thermal analyzer. The samples were placed in a Pt crucible and heated at $3^\circ C\,min^{-1}$ under $100\,ml\,min^{-1}$ air or N_2 flow. The reference was an empty Pt crucible.

Elemental analyses were performed by the Service Central d'Analyse (CNRS, Vernaison, France), using inductively coupled plasma/atomic emission spectroscopy (ICP/AES).

3. Results

3.1. Characterization of the precursor complex

In order to characterize the molecular-level speciation of Pt and Sn in supported catalyst systems, a necessary preliminary step was to obtain extensive data on to the bulk complex salt used as precursor.

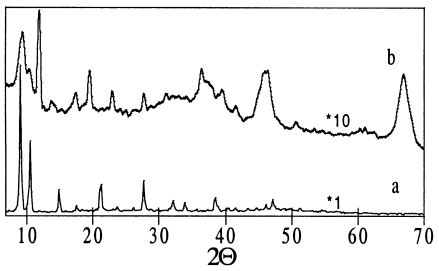

Fig. 1. X-ray diffraction pattern of: (a) the precursor $[(CH_3)_4]_3[Pt(SnCl_3)_5]$, (b) a $[(CH_3)_4]_3[Pt(SnCl_3)_5]/\gamma_c$-$Al_2O_3$ catalyst with 3 wt.% Pt, just after deposition.

Elemental analysis confirmed the stoichiometry expected for $[(CH_3)_4N]_3[Pt(SnCl_3)_5]$: 12.57 wt.% Pt (12.51 calculated), 37.53 wt.% Sn (37.41 calculated) and 34.2 wt.% Cl (34.16 calculated). The XRD pattern (Fig. 1a) is well-defined although it does not seem to have been previously reported.

The diffuse reflectance UV–visible spectrum shows three bands at $\lambda = 500$, 380 and 280 nm, that can be assigned to the d–d transitions of Pt^{II} [25].

NMR spectroscopy of ^{119}Sn and ^{195}Pt, in acetone solutions and in the solid state (MAS), gave the same results as published in previous reports by Pregosin and Rüegger [26] or Shitova et al. [27]. The ^{195}Pt NMR spectrum shows one signal centered at $\delta = -5902$ ppm (not shown) and the ^{119}Sn NMR spectrum one signal at $\delta = -128$ ppm (Fig. 2). Different J couplings can clearly be observed: $^1J(^{195}Pt–^{119}Sn) = 16\,027$ Hz and $^2J(^{195}Pt–^{117}Sn) = 15\,387$ Hz (not shown, relative to ^{195}Pt NMR), which confirms the existence of Pt–Sn bonds, and $^2J(^{119}Sn–^{117}Sn) = 6212$ Hz.

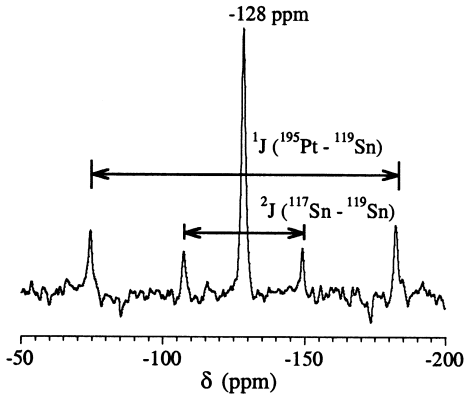

Fig. 2. ^{119}Sn NMR spectrum of the $[(CH_3)_4]_3[Pt(SnCl_3)_5]$ complex in acetone, [Pt]=1.5*10^{-2} M.

Thermal transformations of $[(CH_3)_4N]_3[Pt(SnCl_3)_5]$ were also studied and found to depend on the pretreatment atmosphere. Under air, a two-step exothermic weight loss was observed with maxima at 260°C and 340°C. Under N_2 or Ar, a two-step loss was also observed, but it was endothermic and occurred at higher temperatures (340°C and 390°C).

Characterization of the resulting products by elemental analysis and XRD indicated that Pt^0 and SnO_2 (cassiterite) are the final products of thermal degradation of the precursor under air. Under inert gas (Ar or N_2), the only solid phase observed was the PtSn alloy niggliite [28]. The stoichiometric ratio of 1:1 in niggliite and 5:1 in the complex precursor show that a large part of Sn must be eliminated in the gas phase upon degradation; indeed, needle-like crystals of $SnCl_2$ were deposited in the cold part of the cell.

3.2. Characterization of the catalysts

The catalysts were studied both after the initial deposition and after calcination.

The 0.5 and 1 wt.% Pt samples generally have similar behaviors and will be referred to as “low-loading”, while the 1.5, 2 and 3 wt.% Pt samples are referred to as “high-loading”.

Immediately after deposition, the elemental analyses for Pt, Sn and Cl coincide in all cases with the stoichiometry of the precursor complex.

In the high-loading samples, a new crystalline phase is observed by XRD after deposition (Fig. 1b), with a diffraction pattern clearly different from that of bulk $[(CH_3)_4N]_3[Pt(SnCl_3)_5]$. In opposition, no phase other than the support is detected in low-loading samples. This is not only due to the sensitivity limit of XRD: the long accumulation times used should have permitted detection of proportional amounts of well-crystallized phases, at least in the 1 wt.% Pt sample, if they had been present. It then appears that the limit of 1–1.5 wt.% Pt constitutes the saturation coverage for well-dispersed species in the present system.

The UV–visible spectra always exhibit two bands at 250 and 215 nm that may be assigned to charge transfer transitions in the alumina support (probably $O^{2-} \rightarrow Al^{3+}$). In addition, for the low-loading samples, three

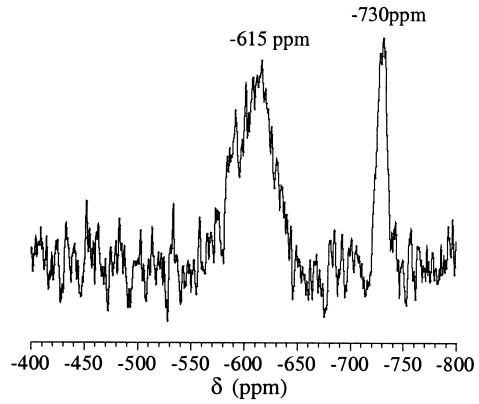

Fig. 3. ^{119}Sn MAS/NMR spectrum of the $[(CH_3)_4]_3[Pt(SnCl_3)_5]$/$\gamma_c$-$Al_2O_3$ with 3 wt.% Pt, immediately after deposition.

additional bands are located at $\lambda = 380$, 320, and 260 nm, i.e., at positions mostly different from those of the bulk precursor. For the high-loading samples, there are also three additional bands, but their maxima are at $\lambda = 500$, 380, and 280 nm, in good correspondence with those of the bulk precursor salt.

All the results mentioned so far would seem to indicate that, while the metal-containing species is significantly modified in low-loading samples (below saturation coverage), some unmodified $[Pt(SnCl_3)_5]^{3-}$ complex ions are still present in high-loading samples (maybe accounting only for the amount in excess of the saturation coverage).

In contrast, the ^{119}Sn NMR spectrum (Fig. 3) is completely different from that of the precursor complex for all of the catalysts studied; the signal at -128 ppm and its satellites have completely disappeared. One broad signal is visible at $\delta = -615$ ppm in all samples while a second and narrower signal at $\delta = -730$ ppm is only observed in the high-loading samples. Thus, the NMR results seem to indicate strong modification of the Sn-containing species in all cases, not just in the high-loading samples. An explanation for this apparent contradiction will be suggested in the discussion.

As regards thermal treatments, calcination of the high-loading samples leads to the formation of phases reminiscent of those observed after bulk compound treatments, i.e., large particles of Pt^0 (average size: 9.7 nm) and SnO_2 (cassiterite) after calcination under air, and niggliite after calcination under Ar or N_2. The TGA traces show two weight loss steps both under air and inert gases. The first step (at temperature as low as 30°C) is simply due to the elimination of the acetone solvent that was adsorbed from the impregnation solution. The second weight loss step has an intensity proportional to the amount of deposited complex; the peak temperatures vary according to the treatment atmosphere, but the integrated weight losses are independent on its nature. Under air, the decomposition reaction is exothermic and occurs at about 330°C, whereas under inert gas it is endothermic and observed at about 280°C.

4. Discussion

4.1. Characterization of the $[(CH_3)_4N]_3[Pt(SnCl_3)_5]$ precursor complex

The spectroscopic signatures of the precursor complex have been clearly established both in UV–visible and NMR.

Bulk $[(CH_3)_4N]_3[Pt(SnCl_3)_5]$ undergoes different thermal transformations according to the nature of the atmosphere with which it is in contact. Due to the uncertainty on the fate of the organic cation, it is difficult to write precise equations for the thermal reactions in absence of mass spectroscopy data. The results presented in Section 3 suggest that decomposition is initiated purely by thermal activation, which could be temporarily written as:

1. $[Pt^{II}(SnCl_3)_5]^{3-} \Leftrightarrow Pt^0 + 5Sn^{II}Cl_2 + 5/2Cl_2 + 3e^-$, with the electrons reducing the organic cation
2. $Pt^0 + Sn^{II}Cl_2 \Leftrightarrow Pt^0Sn^0 + Cl_2$

Only a small part of the $Sn^{II}Cl_2$ formed in reaction (1) is used to form the PtSn alloy, the remainder being lost to the gas phase.

If oxygen is available in the gas phase, a different evolution for $SnCl_2$ is likely to take place:

$$Sn^{II}Cl_2 + O_2 \Leftrightarrow SnO_2 + Cl_2$$

4.2. Characterization of the catalysts

One well-substantiated conclusion that emerges from our data is the existence in this system of a

saturation coverage for the precursor on the alumina surface; below this coverage, only well-dispersed species are formed, while above it, the excess amount of precursor forms a separate phase detected by XRD. The limit lies somewhere between 1 and 1.5 wt.% Pt, corresponding to 0.16–0.25 Pt atoms/nm^2 (or 0.82–1.22 Sn atoms/nm^2). An approximate estimate of the loading corresponding to one physical monolayer of $[(CH_3)_4N]_3[Pt(SnCl_3)_5]$, using a modeling program, would yield about 1.5 molecules of complexes per square nanometer; in spite of the uncertainty inherent in such calculations, it seems clear that the saturation coverage is about an order of magnitude smaller than a physical monolayer. It is not obvious at this point what features of the surface contribute to determine the saturation coverage, especially since the mechanism of "alumina-precursor" interaction is not precisely known.

Let us consider now the chemical nature of both species (which we will refer to, for the time being, as the "low-loading" and the "high-loading" species). We have already mentioned an apparent contradiction: UV–visible spectroscopy indicates that the high-loading species has electronic transitions similar to those of the bulk compound (while those of the low-loading species are different), so that one might believe that it merely consists of unmodified $[Pt(SnCl_3)_5]^{3-}$ complexes. However, this is not compatible with ^{119}Sn NMR data, which shows that the low-loading and high-loading species have distinct spectroscopic signatures, in a range of chemical shifts (-615 and -720 ppm, respectively) completely different from that where the ^{119}Sn resonances are found in $[Pt(SnCl_3)_5]^{3-}$.

The data may be reconciled if one considers that the electronic transitions at 500, 380, and 280 nm probed by UV–visible spectroscopy concern orbitals centered on Pt, and therefore are mostly influenced by the molecular environment of Pt atoms, while ^{119}Sn NMR probes the environment of Sn atoms. We can then account for all observations if we propose that: (i) in the low-loading species, both the coordination sphere of Pt and that of Sn are strongly modified with respect to the precursor complex, (ii) in the high-loading species, the coordination sphere of Pt is unaffected while that of Sn is modified.

^{119}Sn chemical shifts allow further insight on the nature of these modifications. Sheng et al. [29] have observed a signal at -600 ppm in Al_2O_3–SnO_2 prepared by co-precipitation but offered no assignment for it. Blunden et al. [30] found $\delta = -612$ ppm for the compound "Sn(O–*n*Bu)$_4$(H$_2$O)$_2$" which has a coordination sphere ($Sn^{IV}O_6$). The low-loading species in our systems could well have the same coordination sphere (with a formula of the type $[Sn(OH)_3(H_2O)_3]^-$), if both the Sn–Cl and Sn–Pt bonds have been hydrolyzed, or maybe $[(AlO)_xSn(OH)_3(H_2O)_{3-x}]^{(x+1)-}$, if hydrolysis is accompanied by grafting to surface groups (however, the fate of Pt in this case remains an open question). As for the high-loading species, the chemical shift value observed, at -720 ppm, is rather close to that of the low-loading species (-615 ppm), suggesting relatively similar coordination spheres for Sn; since we have reason to believe that Pt–Sn bonds are preserved, we tentatively assign this chemical shift to a partially hydrolyzed species of the type $[Pt\{Sn(OH)_3(H_2O)_2\}_5]^{3-}$. Experiments on the controlled hydrolysis of the bulk precursor complex are underway to confirm this assignment.

For both species proposed above, water must be supplied to cause the extensive precursor hydrolysis that is postulated. Since deposition was carried out from a non-aqueous solvent, its most likely source is the incompletely dehydrated alumina surface, or maybe even the bulk alumina which is known to act as a "water-sponge" [31].

The thermal behavior of low-loading species has not been well-characterized so far (the availability of Mössbauer data should soon allow to follow the evolution of the Sn environment). As regards the high-loading species, it seems that its transformations are closely related to those of the bulk complex as the same final phases are observed: Pt^0 and SnO_2 after treatment under air, and niggliite (PtSn alloy) after treatment under inert gas. It should be recalled that the low-loading species is present in all samples (the high-loading species being superimposed to it) and remains well-dispersed: EDX analysis of thermally treated samples, in areas where no large Pt or Sn particles were visible, did indeed reveal strong Sn–Pt signals. These well-dispersed metal species are likely to play an important role in the final properties of the supported catalysts, and a systematic study of the chemisorptive and catalytic properties of these sys-

tems is currently being carried out. The present results already show that the intermediate formation of SnO_2, for instance, is an important factor in catalyst evolution: those samples where bulk SnO_2 has been formed as an intermediate species show a much reduced accessibility of Pt particles (as measured by H_2 chemisorption and H_2–O_2 double titration) at a later stage, probably due to a kind of SMSI effect. Therefore, the approach we have followed, based on the systematic characterization of Pt and Sn species after each step of catalyst preparation, appears well-suited to rationalize the final properties of supported Pt–Sn catalysts and evaluate the corresponding key synthesis parameters.

5. Conclusions

Deposition of the $[(CH_3)_4N]_3[Pt(SnCl_3)_5]$ precursor onto alumina leads to two different types of surface species according to the metal loading. Under 1 wt.% Pt, the deposited species are well-dispersed on the surface and it seems that Pt–Sn bonds are not preserved. For higher Pt loadings, a bulk phase is formed, containing complexes where the Pt–Sn bonds are apparently preserved, but the Sn–Cl bonds are partly or totally hydrolyzed.

This difference in speciation as a function of Pt loading constitutes a first way to control the intimacy of the Pt/Sn interaction, and hence the properties of the final catalyst. Another easily applicable tool may be the nature of the atmosphere used for thermal treatments, since for high-loading samples, just as for the bulk precursor compound, the use of an oxidizing atmosphere results in demixtion (formation of two distinct phases, Pt^0 and SnO_2) while the use of a neutral atmosphere favors an intimate Pt–Sn interaction (formation of the PtSn alloy). In any case, a molecular characterization of the metallic species formed after each step of synthesis is required in order to optimize the catalyst synthesis procedure.

Acknowledgements

The authors are grateful to S. Gautier for his help in acquiring ^{119}Sn NMR spectra. C.A. acknowledges a Ph.D. grant from the French Ministry of National Education.

References

[1] J.H. Sinfelt, Bimetallic Catalysts: Discoveries, Concepts, and Applications, Wiley, New York, 1983.
[2] E.M. Blue, Hydrocarb. Process 48 (1969) 141.
[3] H.E. Kluksdahl, US Patent 3 415 737 (1968).
[4] J.H. Sinfelt, US Patent 3 953 368 (1976).
[5] F.M. Dautzenberg, Patent German Offenlegungsschrift 2 121 765 (1971).
[6] F.M. Dautzenberg, Patent German Offenlegungsschrift 2 153 891 (1972).
[7] F.C. Wilhelm, US Patent 3 844 938 (1974).
[8] V.N. Seleznev, Y.V. Formichev, M.E. Levinter, Neftekhimiya 14 (1974) 205.
[9] F.M. Dautzenberg, J.N. Helle, P. Biloen, W.M.H. Sachtler, J. Catal. 63 (1980) 119.
[10] P. Biloen, J.N. Helle, H. Verbeek, F.M. Dautzenberg, W.M.H. Sachtler, J. Catal. 63 (1980) 112.
[11] R. Burch, J. Catal. 71 (1981) 348.
[12] R. Gomez, V. Bertin, T. Lopez, I. Schifter, G. Ferrat, J. Mol. Catal. A 109 (1996) 55.
[13] F. Bettcher, P. Chaumette, B. Didillon, O. Clause, Stud. Surf. Sci. Catal. 92 (1994) 131.
[14] Z. Paal, A. Gyory, I. Uszkurat, S. Olivier, M. Guérin, C. Kappenstein, J. Catal. 168 (1997) 164.
[15] A. El Abed, S. El Qebbaj, M. Guérin, C. Kappenstein, M. Saouabe, P. Marecot, J. Chim. Phys. 92 (1995) 1307.
[16] G.T. Baronetti, S.R. de Miguel, O.A. Scelza, M.A. Fritzler, A.A. Castro, Appl. Catal. 19 (1985) 77.
[17] G.T. Baronetti, S.R. de Miguel, O.A. Scelza, A.A. Castro, Appl. Catal. 24 (1986) 109.
[18] S.R. de Miguel, G.T. Baronetti, A.A. Castro, O.A. Scelza, Appl. Catal. 45 (1988) 61.
[19] J. Llorca, P.R. de la Piscina, J.-L.G. Fierro, J. Sales, N. Homs, J. Mol. Catal. A 118 (1997) 101.
[20] R. Srinivasan, R.J. de Angelis, B.H. Davis, J. Catal. 106 (1987) 449.
[21] G. Martino, Stud. Surf. Sci. Catal. 4 (1980) 399.
[22] Y.L. Yermakov, B. Kuznetsov, V.A. Zakharov, Stud. Surf. Sci. Catal. 8 (1981) 356.
[23] X. Li, Y. Wei, J. Cheng, R. Li, Stud. Surf. Sci. Catal. 75 C (1993) 2407.
[24] P.G. Antonov, Y.N. Kukushkin, V.G. Shtrele, Y.P. Kostikov, F.K. Egorov, Russ. J. Inorg. Chem. 27 (1982) 1770.
[25] A.B.P. Lever, Inorganic Electronic Spectroscopy, 2nd Edition, Stud. Phys. Theor. Chem., Vol. 33, Elsevier, Amsterdam, 1984, 544 pp.
[26] P.S. Pregosin, H. Rüegger, Inorg. Chim. Acta 86 (1984) 55.
[27] N.B. Shitova, L.Y. Alt, V.I. Perevalova, A.S. Belyi, V.K. Duplyakin, React. Kinet. Catal. Lett. 23 (1983) 17.
[28] C. Harris, Mineral. Mag. 38 (1972) 174.
[29] T.-C. Sheng, P. Kirszensztejn, T.N. Bell, I.D. Gay, Catal. Lett. 23 (1994) 119.
[30] S.J. Blunden, D. Searle, P.J. Smith, Inorg. Chim. Acta 116 (1986) L31.
[31] K. Sohlberg, S.J. Pennycook, S.T. Pantelides, J. Am. Chem. Soc. 121 (1999) 7493.